

The transformation from 2°-amine to 3°-amine of cyclam ring alter the fragmentation patterns of 1-tosylcytosine-cyclam conjugates

Renata Kobetić^{a*}, Valentina Ključarić,^b Dijana Saftić,^a Josipa Matic, ^a Željka Ban,^a Snježana Kazazić^c and Biserka Žinić^{a*}

^aLaboratory for Biomolecular Interactions and Spectroscopy, Division of Organic Chemistry and Biochemistry, Ruđer Bošković Institute, Bijenička cesta 54, 10 000 Zagreb, Croatia

^bMinistry of Defense of the Republic of Croatia, Dr. Franjo Tuđman Croatian Defense Academy, Ilica 256 b, Zagreb, Croatia

^cLaboratory for Mass Spectrometry, Division of Physical Chemistry, Ruđer Bošković Institute, Bijenička cesta 54, 10 000 Zagreb, Croatia

Key words: cyclam conjugate; *N*-1-tosylcytosine; Cu²⁺ and Zn²⁺ complexes; ring stability; ESI-MS, fragmentation reactions

Running title: 1-tosylcytosine-cyclam conjugates

Correspondence to: Renata Kobetić; E-mail: rkobetic@irb.hr; Phone: **385-1-4561111 ext. 1775; Fax: **385-1-4680195; Biserka Žinić, E-mail: bzinic@irb.hr; Phone: **385-1-4561066

ABSTRACT

The novel *N*-1-sulfonylcytosine-cyclam conjugates **1** and **2** conjugates are ionized by electrospray ionization mass spectrometry (ESI MS) in positive and negative modes (ES⁺ and ES⁻) as singly protonated/deprotonated species or as singly or doubly charged metal complexes. Their structure and fragmentation behavior is examined by collision induced experiments (CID). It was observed that the structure of the conjugate dictated the mode of the ionization: **1** was analyzed in ES⁻ mode while **2** in positive mode. Complexation with metal ions did not have the influence on the ionization mode. Zn²⁺ and Cu²⁺ complexes with ligand **1** followed the similar fragmentation pattern in negative ionization mode.

The transformation from 2°-amine to **1** to 3°-amine of cyclam ring in **2** lead to the different fragmentation patterns due to the modification of the protonation priority which changed the fragmentation channels within the conjugate itself. Cu²⁺ ions formed complexes practically immediately and the priority had the cyclam portion of the ligand **2**. The structure of the

This article has been accepted for publication and undergone full peer review but has not been through the copyediting, typesetting, pagination and proofreading process which may lead to differences between this version and the Version of Record. Please cite this article as doi: 10.1002/jms.4197

formed Zn^{2+} complexes with ligand **2** depended on the number of 3° amines within the cyclam portion of the conjugate and the ratio of the metal: ligand used. The cleavage of the cyclam ring of metal complexes is driven by the formation of the fragment that suited the coordinating demand of the metal ions and the collision energy applied. Finally, it was shown that the structure of the cyclam conjugate dictates the fragmentation reactions and not the metal ions.

INTRODUCTION

The nucleoside analogues are a large class of agents used as antiviral agents or drugs for cancer (cytarabine, gemcitabine, mercaptopurine), rheumatologic diseases (azathioprine, allpurinol) and even bacterial infections (trimethoprim). Due to their wide spectrum of applicability in medicine there is a continuous attempt to prepare new drug candidates with novel modes of action against drug-resistant microorganisms. Our group has a long-term experience in design, synthesis and characterization of nucleoside derivatives. We have described the synthesis of novel *N*-1-sulfonylpyrimidine derivatives¹⁴ which showed strong antitumor activity in *in vitro*⁵⁻⁸ and *in vivo*⁹⁻¹¹ conditions. Inspired by the numerous reports on the antitumor activity of metal complexes,^{12,13} we prepared *N*-1-sulfonylpyrimidine metal complexes.¹⁴ *N*-1-sulfonylcytosine is capable to form palladium (II)^{15,16} and other transition metal complexes including Cu(II)¹⁷. In addition, we studied their interactions with biologically important cations using electrospray ionization mass spectrometry (ESI-MS).¹⁸ To further explore the biological potential of this type of molecules, their structure was modified by combining them with cyclam^{19,20}, which strongly binds a wide range of metal ions forming complexes known for their antiviral activity.^{21,22} Recently, a new class of nontoxic metal-cyclam complexes (Cu^{2+} and Zn^{2+}) was prepared with potency against drug-resistant mycobacterium tuberculosis.²³ These results motivated us to prepare also Cu^{2+} and Zn^{2+} complexes of our novel conjugates. Despite of the biological importance of this type of molecules, detailed gas phase study and fragmentation reactions are few. This is surprising considering the fact that the fragmentation reactions using ionization mass spectrometry are an important tool for the structural elucidation and characterization of synthetic and natural products. In the past, mass spectrometry was often used for the characterization of new metal complexes with cyclam as valuable ligand.²⁴ Besides the systematic analysis of the complex formation with alkali and transition-metal ions,²⁵ the protonation behavior of a cyclam derivative with different acids was studied likewise.²⁶ Ion mobility mass spectrometry was

used in order to elucidate the gas-phase structures.²⁷ However, a detailed analysis of the collision induced fragmentation (CID) reactions of cyclam derivatives and their corresponding metal complexes in the highly diluted gas phase has been carried out only in a couple studies. One of them was Schalley's studies of fragmentation reaction of thiourea and sugar-substituted cyclams and their transition metal complexes.²⁸ The fragmentation occurred within the side chains through a number of different 1,2-elimination reactions irrespective of the absence or presence of a transition metal ion such as Co^{2+} , Ni^{2+} , or Zn^{2+} . A remarkable exception was Cu^{2+} , which induced ring cleavage reactions. This was traced back to an electron transfer from the cyclam nitrogen atoms to the Cu^{2+} ion. The electron transfer created a cation or anion-radical within the macrocycle, which induced typical fragmentation reactions that lead to fragmentation within the macrocycle.

The focus of this report is on the detailed MS/MS analysis of the collision induced fragmentation reactions of novel *N*-1-sulfonylcytosine-cyclam conjugates **1** and **2** (Figure 1) and their Cu^{2+} and Zn^{2+} complexes. The metal ion position and the structures of the formed complex ions were determined. The attention was paid to the effect of the *N*-substitution of macrocycle (2° or 3° amine) and metal ion in regard to the stability of the ring metal complexation in condensed phase towards the gas phase and possible correlation of the obtained results. The studies were performed in positive and negative modes and major fragmentation reactions were compared. The idea was to prove the effect of substituents and metal ions towards the complex formation and fragmentation patterns of conjugates **1** and **2**.

EXPERIMENTAL

Synthesis

N-1-tosylcytosine **3** was synthesized by condensation of cytosine and *p*-toluenesulfonylchloride (TsCl).⁹ The synthesis of 5-morpholinomethylcytosine²⁹ and 5-morpholinomethyl-*N*1-tosylcytosine³⁰ was described earlier via an acid catalyzed Mannich reaction of cytosine/*N*1-tosylcytosine with paraformaldehyde and morpholine in ethanol. The Mannich reaction of **3** with cyclam **4** and paraformaldehyde in the presence of acetic acid yielded *C*-aminomethylated conjugate **1** in which the cyclam was attached at C5 position of cytosine by methylene bridge. The same reaction with protected cyclam³¹ **5** gave *N*-aminomethylated product **2** (Scheme 1). Aminomethylation of the cytosine at C4 position has already been reported in the analogous reaction with morpholine and formaldehyde.³²

General: TLC was carried out on DC-plastikfolien Kieselgel 60 F254 and preparative thick-layer (2 mm) chromatography was done on Merck 60 F254 (Merck KGaA, Darmstadt, Germany). ^1H and ^{13}C NMR spectra were recorded in $\text{DMSO-}d_6$ with a Varian Gemini 300 (300/75 MHz) spectrometer using $\text{DMSO-}d_6$ as the internal standard. Microwave assisted synthesis was conducted in a borosilicate glass vial sealed by reusable snap-cap with polytetrafluoroethylene (PTFE) coated silicone septum. The microwave heating was performed in the Anton Paar microwave synthesis reactor Monowave 300 (Anton Paar® GmbH, A-8054 Graz, Austria). Reaction mixture was stirred with a magnetic stir bar during the irradiation. The temperature, pressure and irradiation power were monitored during the course of the reaction. After completed irradiation, the reaction tube was cooled with high-pressure air until the temperature had fallen below $55\text{ }^\circ\text{C}$ (*ca.* 1 min).

N-1-tosylcytosine-cyclam conjugate 1

To a suspension of *N*-1-tosylcytosine **3** (200.5 mg, 0.75 mmol), cyclam **4** (300.5 mg, 1.50 mmol) and paraformaldehyde (46.3 mg, 1.54 mmol) in ethanol (5 mL) concentrated acetic acid (172 μL , 3 mmol) was added. The suspension was irradiated at $100\text{ }^\circ\text{C}$ for 30 min in the microwave cavity. After evaporation of solvent, the residue was purified by preparative chromatography $\text{CH}_2\text{Cl}_2/\text{MeOH}$ (3:1) yielding **1** (54 mg, 15 %) as a white powder: ^1H NMR (600 MHz, $\text{DMSO-}d_6$) δ/ppm : 8.45 (s, 1H, H-6), 7.62 (d, 2H, $J = 8.0\text{ Hz}$, Ts-b), 7.14 (d, 2H, $J = 8.0\text{ Hz}$, Ts-c), 4.26–3.20 (m, NH-cyclam + $\text{NH}_2 + \text{H}_2\text{O}$), 3.16 (s, 2H, C5- $\text{CH}_2\text{-N}$), 2.95–2.66 (m, 12H, $\underline{\text{CH}_2}\text{-NH-cyclam}$), 2.30 (m, 4H, $\text{CH}_2\text{-cyclam}$), 2.04 (s, 3H, CH_3), 1.86 (m, 2H, $\text{CH}_2\text{-}\underline{\text{CH}_2}\text{-CH}_2$), 1.69 (m, 2H, $\text{CH}_2\text{-}\underline{\text{CH}_2}\text{-CH}_2$); ^{13}C NMR (75 MHz, DMSO) δ/ppm : 167.90 (s, C-4), 162.37 (s, C-2), 144.26 (s, Ts-d), 138.91 (s, Ts-a), 131.43 (d, C-6), 128.04 (d, Ts-c), 126.63 (d, Ts-b), 72.41 (s, C-5), 68.87 (t, C5- $\text{CH}_2\text{-N}$), 53.30 (t, $\text{CH}_2\text{-cyclam}$), 52.54 (t, $\text{CH}_2\text{-cyclam}$), 51.62 (t, $\text{CH}_2\text{-cyclam}$), 50.79 (t, $\text{CH}_2\text{-cyclam}$), 49.01 (t, $\text{CH}_2\text{-cyclam}$), 48.58 (t, $\text{CH}_2\text{-cyclam}$), 46.54 (t, $\text{CH}_2\text{-cyclam}$), 45.46 (t, $\text{CH}_2\text{-cyclam}$), 25.87 (t, $\text{CH}_2\text{-}\underline{\text{CH}_2}\text{-CH}_2$), 23.62 (t, $\text{CH}_2\text{-}\underline{\text{CH}_2}\text{-CH}_2$), 20.89 (q, CH_3). ESI-MS: m/z calcd. for $\text{C}_{22}\text{H}_{34}\text{N}_7\text{O}_3\text{S}$ [M-H] 476.25, found 476.10.

N-1-tosylcytosine-tri-(trifluoroacetyl)cyclam conjugate 2

To a suspension of *N*-1-tosylcytosine **3** (200.5 mg, 0.75 mmol), tri-(trifluoroacetyl)cyclam **5** (732.2 mg, 1.50 mmol) and paraformaldehyde (46.3 mg, 1.54 mmol) in ethanol (5 mL)

concentrated acetic acid (172 μ L, 3 mmol) was added. The suspension was irradiated at 100 $^{\circ}$ C for 30 min in the microwave cavity. The resulting solid was filtered off, the filtrate was evaporated and the residue was purified by preparative chromatography $\text{CH}_2\text{Cl}_2/\text{MeOH}$ (3:1) yielding **2** (76 mg, 27 %) as a white powder: ^1H NMR (300 MHz, $\text{DMSO-}d_6$) δ /ppm: 9.03–8.49 (br. s, 1H, NH), 8.30–7.99 (m, 1H, H-6), 7.97–7.70 (m, 2H, Ts-b), 7.46–7.41 (m, 2H, Ts-c), 6.12–5.93 (m, 1H, H-5), 4.27–3.94 (br. d, 2H, C5- $\underline{\text{CH}_2}$ -N), 3.86–3.21 (m, 12H, N- CH_2 -NH + H_2O), 2.66–2.64 (m, 2H, CH_2 -cyclam), 2.46–2.31 (br. s, 3H, CH_3), 1.98 (m, 2H, CH_2 - $\underline{\text{CH}_2}$ - CH_2), 1.84–1.55 (m, 2H, CH_2 - $\underline{\text{CH}_2}$ - CH_2); ^{13}C NMR (75 MHz, $\text{DMSO-}d_6$) δ /ppm: 164.56 (C-4, multiplets due to existence of conformers), 157.07–155.43 (m, CF_3 - $\underline{\text{C}}=\text{O}$), 150.77 (br. s, C-2), 145.37 (br. s, Ts-d), 138.94 (br. d, C-6), 133.92 (br. s, Ts-a), 129.48 (d, Ts-c), 128.99–128.80 (m, Ts-b), 121.61–113.98 (quartet, CF_3 , due to C-F coupling, $J_{\text{C,F}}\sim 260$ Hz, further split due to existence of conformers), 97.52 (br. d, C-5), 58.66–56.93 (m, N- CH_2 -N), 52.88–43.53 (m, CH_2 -N), 28.38–23.38 (m, CH_2 - $\underline{\text{CH}_2}$ - CH_2), 21.04 (q, CH_3). ESI-MS: m/z calcd. for $\text{C}_{28}\text{H}_{33}\text{F}_9\text{N}_7\text{O}_6\text{S}$ $[\text{M}+\text{H}]^+$ 766.25, found 766.20.

ESI-MS

General

The solvents used for the spectroscopic measurements were HPLC or spectroscopic grade (Sigma-Aldrich Chemie GmbH, Steinheim, Germany) and were used without further purification. Salts: $\text{ZnSO}_4\cdot 7\text{H}_2\text{O}$ and $\text{CuCl}_2\cdot 2\text{H}_2\text{O}$, were purchased (Sigma-Aldrich Chemie GmbH, Steinheim, Germany) and were used without further purification.

Instrumentation

The MS analysis was conducted by electrospray ionization, and the spectra were obtained at the same concentrations in both the ES^+ and ES^- modes. Certain ligand and complex fragmentations occurred at higher collision energies (for example: Agilent 6420 range 5-40 eV). The masses of the complexes reported in this paper are the masses containing the most abundant, stable isotope of each element in a complex.³³ The spectra were recorded and compared under the same MS conditions.

1. The mass spectral data were acquired using an Agilent 6420 Triple Quad mass spectrometer equipped with an electrospray ionization (ESI) interface operated in the positive

and negative ion modes (Agilent Technologies, Palo Alto, CA, USA). Stock samples were prepared in methanol. Stock solutions were further diluted to a concentration of approximately 0.05 mg/mL and directly injected. The infusion into the mass spectrometer was performed at a flow rate of 3 $\mu\text{L}/\text{min}$. Nitrogen was used as an auxiliary and sheath gas. The spray voltage was set at 4.5 kV. The capillary temperature was 150–300 $^{\circ}\text{C}$, and the voltage range of the collision cell was 80–180 V. The full mass spectra were acquired over the mass range m/z 10–2000. For data acquisition and analysis Mass Hunter software (Agilent Technologies, Inc. 2006–2007) was used. A parent ion window of typically 4 amu (i.e., parent mass ± 2 amu) was chosen to perform further MS/MS experiments.

2. The mass spectral data were also acquired using an LCQ Deca ion trap mass spectrometer from ThermoFinnigan (San Jose, CA, USA) equipped with an electrospray ionization (ESI) interface operated in the positive and negative ion modes. Stock samples were prepared in methanol. Stock solutions were further diluted to a concentration of approximately 0.05 mg/mL and directly injected. The infusion into the mass spectrometer was performed by the built-in syringe pump at a flow rate of 5 $\mu\text{L}/\text{min}$. Nitrogen was used both as an auxiliary and sheath gas. Helium was used as the collision gas in the ion trap. The sheath gas flow was set at 85 and the auxiliary gas flow at 30 (arbitrary units). The spray voltage was set at 4.5 kV, while the capillary temperature was 250 $^{\circ}\text{C}$ and the capillary voltage 17 V. The full mass spectra were acquired over the mass range m/z 150–2000.

For the MS/MS investigations, characteristic molecular ions were isolated in the ion trap and collision activated with different collision energies (CE) to find the optimal CE for distinct fragmentation. The product ions in the MS/MS spectra were chosen for further MS^3 and MS^4 experiments by selecting a parent ion window of typically 2 amu (i.e., parent mass ± 1 amu).

3. The ESI MS^n ($n > 2$, a parent ion window of typically 2 amu (i.e., parent mass ± 1 amu)) experiments were recorded using an amaZon ETD mass spectrometer (Bruker Daltonik, Bremen, Germany) equipped with the standard ESI ion source (the nebulizer pressure: 8 psi; the drying gas flow rate: 5 L/min; the drying gas temperature: 250 $^{\circ}\text{C}$). The mass spectrometer was operated in the positive and negative polarity modes, and the potential on the capillary cap was $-/+$ 4500 V. Helium was used as a collision gas. The stock solutions of the compounds were diluted in methanol to a concentration of approximately 0.5×10^{-6} mol/dm³ and injected into the ESI source of the mass spectrometer by a syringe pump at a flow rate of 1 $\mu\text{L}/\text{min}$.

RESULTS AND DISCUSSION

A brief overview of the MS profile of the ligands **1**, **2** is given first, followed by the elucidation of the structure of the new species formed due to their interactions with metal ions Zn^{2+} and Cu^{2+} . Molecular complexes with Cu^{2+} and ionic complexes with Zn^{2+} were observed. The differences in the formation rate of complexes were observed as well. The detected fragmentation for Cu(II) complexes with ligands **1** and **2** followed processes described by Schalley for the thiourea- and sugar-substituted cyclams and their Cu (I or II) complexes²⁸. The transition metals induced fragmentation reactions, very similarly as compared to the protons and could be classified mainly as Lewis acids.

We observed that the complexation of conjugate **1** with both metal ions (Cu^{2+} and Zn^{2+}) dictated the place of collision induced cleavage of the cyclam ring. The transformation from 2°-amine to 3°-amine of cyclam ring in **2** lead to different fragmentation patterns due to the modification of the protonation priority - the alteration of the intrinsic properties (electronic, inductive, steric, vibrational) caused the switch in the fragmentation patterns within the conjugate itself.

The main difference between Cu^{2+} and Zn^{2+} complexes with **2** is that only Zn^{2+} ions formed complexes with “broken” conjugate **2**.

Cyclam derivatives

The two main variations under study were the number of the substituents on cyclam ring and the scanning mode. The modification of cyclam ring to have all 3°-amines as potential ligands changed the stability of the ring towards the induced fragmentation and the ability to bind the metal ions.

The ligand **1** had mono substituted cyclam ring which fragmented already at the source in positive mode. It was not observed any signals corresponding to the whole ligand in ES^+ spectrum but rather contained fragment, **F**, (Scheme 2) formed due to the cyclam ring cleavage; e.g. its H^+ adduct observed at m/z 409.9 respectively its dimer Na^+ adducts at m/z 841.1; 863.1 or 885.1. On the other hand, the signal of molecular ion was present as deprotonated signal at m/z 476.6 in the ES^- mass spectrum of **1** but still the dominant was the signal of fragment **F** as sodium dimer adduct at m/z 839.3 Figure 2. The collision-induced dissociation experiments of the $[\mathbf{1-H}]^-$ ions were performed. The ring fragmentation pathways were observed pointing to the radical fragmentation mechanisms to dominate in channels (Scheme 2).

Compound **1** contained three 2°-amine and one 3°-amine within the cyclam ring and therefore, most likely the protonation occurred within cyclam macrocycle cavity at the tertiary nitrogen atom which (at least in the gas phase) – could have higher proton affinity than the primary group of the cytosine moiety.³⁴ This fact led to the cleavage of the compound already at the source. Therefore, the compound **1** was analyzed in negative mode because the 2°-amine is stronger Lewis acid than the primary amine and the initial deprotonation occurred much easier and energetically far less costly from any of three 2°-amines. The introduction of the substituent to the ring (all 3°-amines in conjugate **2**) changed the position of the initial protonation and there was no 2°-amine available for the deprotonation of the nitrogen within the ring; therefore, the fragmentation of **2** proceeded through several channels in positive mode, out of which two channels were major (Scheme 3). One channel progressed through radical fragmentation reactions (path A) and the second through charge migration fragmentation reaction (CMF) (path B) in positive ions. It is not a surprise since carbonyl functions in structures lead to the inductive cleavages assisted by adjacent heteroatoms, observed mainly in esters, amides or carboxylic acids.³⁵

Collision-induced fragmentation of signal m/z 839.0 assigned as sodium dimer adduct of fragment **F** proceeded through one channel analog to the deprotonated monomer **1**, yielding signal at m/z 408.5 (**F**). Again, the cyclam ring broke down producing stable structure **F** which fragmentation followed the same pathway shown on Scheme 2.

Complexes with Cu^{2+}

Both ligands **1** and **2** formed molecular complexes with the $CuCl_2$ (imbedded spectra in scheme 4 respectively 5 for molecular ions) There was not a significant difference in the fragmentation processes of either complex. Copper complex with ligand **1** fragmented through two major fragmentation channels *via* the radical mechanism, Scheme 4.

Ligand **2** with all substituted 3° amines formed complexes with Cu^{2+} that require higher collision energies to fragment through the radical mechanism (red path), Scheme 5. It is interesting that the protonated molecular complex detected as signal at m/z 899.0 fragmented mainly via radical mechanism and that the ring cleavage occurred before tosyl or $-COCF_3$ group departure.

The cyclam coordinative bond N-Cu broke primarily and the cyclam ring remained untouched at lower CE (blue path), Scheme 5. The fragmentation was channeled in two directions: 1. $\text{Cu}^{2+}/\text{CuCl}^+$ departure (mainly) and 2. the departure of HCl. The complex ion (signal at m/z 863.1) was present at lower CE because the sufficient chelate effect discouraged metal ion dissociation from the complex and the signal disappeared by increase of the CE. The ring cleavage and the metal ion departure occurred at higher CE. The major fragmentation channel preceded further through radical (signal at m/z 471.0) mechanism via the ring cleavage, Scheme 5.

Complexes with Zn^{2+}

Compound **1** complexed Zn^{2+} ion within the ring, analog to the Cu^{2+} ion and the fragmentation in negative mode preferentially occurred within the ring following almost the same paths. Precursor ions for each complex were different. Single-charged molecular ion of Cu^{2+} complex was observed as signal at m/z 573 (scheme 4). Two molecules of conjugate **1** coordinated Zn^{2+} ion forming complex ion detected as single-charged molecular ion at m/z 1033 in the gas phase. First fragmentation step yielded single-charged ion observed at m/z 537.9 for Cu^{2+} complex and at m/z 539.1 for Zn^{2+} complex. The structures of both complex ions were analog and the fragmentation channels from that point followed the same paths, Scheme 6 and Figure 3. It could be seen also that the collision induced dissociation caused sequential H_2 loses for both kind of complex ions at the same applied experimental conditions. The abundances of formed species and the level of the H_2 eliminations were different.

Conjugate **2** formed the mixture of the ionic complexes with Zn^{2+} ions in the condensed phase. The composition of the complexes depended on the reaction time and the ratio between Zn^{2+} ions and macrocycle **2**. The formation of the complexes was slow (several days) and the cleavage of the cyclam ring in condensed phase was observed especially if the excess of metal ions was used. The formation of the complexes was followed by the appearance of the signals belonged to the complex ions. It could be seen that the major complex ion was one with signal m/z 377.1 obtained when 1:1 ratio between Zn^{2+} and compound **2** was used, whereas the major complex ion observed as signal m/z 421.1 formed at 2:1 ratio between Zn^{2+} and compound **2**, Figure 4. Namely, lengthening the interaction

time promoted the elimination of the substituents from the ring leading by N-1-tosilcytosine followed by $-\text{COCF}_3$ group.

Additionally, the variation of the energy for the collision induced dissociation caused sequential H_2 losses observed from the single charged complexes, Figure 5.

CONCLUSIONS

Both metal ions, Cu^{2+} and Zn^{2+} , formed complexes with cyclam portions of the conjugate **1**. The signals which belonged to the coordination of Cu^{2+} with the cytosine portion of the ligand and/or cyclam were observed only when higher ratio of Cu^{2+} was used. In general, CID cause the cleavage of the C-C bond nearest the nitrogen in alkylamines yielding an alkyl radical and nitrogen containing cation. We observed that the complexation of conjugate **1** with both metal ions (Cu^{2+} and Zn^{2+}) dictated the place of collision induced cleavage.

The transformation from 2°-amine to 3°-amine of cyclam ring in **2** lead to different fragmentation patterns due to the modification of the protonation priority which changed the fragmentation channels within the conjugate itself. Cu^{2+} ions formed complexes practically immediately and the priority had cyclam portion of the ligand **2** again. The structure of the formed Zn^{2+} complexes with ligand **2** depended on number of 2° or 3° amines within the cyclam portion of the conjugate and the ratio of the metal : ligand used. The formation of the complex was slow (several days) and the ring cleavage of the cyclam in condensed phase was observed if the excess of metal ions was used. The main difference between Cu^{2+} and Zn^{2+} complexes with **2** is that only Zn^{2+} ions formed complexes with “broken” conjugate **2**.

Finally, it was shown in this report that the structure of the cyclam conjugate dictates the fragmentation reactions and not the metal ion necessarily as described previously in literature.²⁸ The place of cleavage is driven by the stability of the fragment that had to suit coordinating demand of the metal ions and the collision energy applied.

Additionally, the variation of the energy for the collision induced dissociation caused sequential H_2 losses observed from the single-charged complex ions at various CE.

ACKNOWLEDGMENTS

This work was supported by the Croatian Ministry of Science, Education and Sport through Grant No. 098-0982914-2935, Croatian Science Foundation Grant No. HRZZ 1447. The

authors would like to acknowledge the contribution of COST Action TD 1304, The Network for the Biology of Zinc (Zinc-Net).

- [1] B. Kašnar, I. Krizmanić, M. Žinić, Synthesis of the sulfonylpyrimidine derivatives as a new type of sulfonylcytoureas, *Nucleos. Nucleot.* **1997**, *16*, 1067–1071.
- [2] B. Žinić, I. Krizmanić, D. Vikić-Topić, M. Žinić, 5-Bromo- and 5-iodo-*N*-1-sulfonylated cytosine derivatives. Exclusive formation of keto-Imino tautomers, *Croat. Chem. Acta.* **1999**, *72*, 957–966.
- [3] B. Žinić, I. Krizmanić, M. Žinić, Sulfonylpyrimidine derivatives with anticancer activity, EP, 0 877 022 B1, 2003.
- [4] D. Saftić, R. Vianello, B. Žinić, 5-Triazolyluracils and Their N^1 -Sulfonyl Derivatives: Intriguing Reactivity Differences in the Sulfonation of Triazole N^1 -Substituted and N^1 -Unsubstituted Uracil Molecules, *Eur. J. Org. Chem.* **2015**, 7695–7704.
- [5] Lj. Glavaš-Obrovac, I. Karner, B. Žinić, K. Pavelić, Antineoplastic activity of novel *N*-1-sulfonylpyrimidine derivatives, *Anticancer Res.* **2001**, *21*, 1979–1986.
- [6] Lj. Glavaš-Obrovac, I. Karner, M. Pavlak, M. Radačić, J. Kašnar-Šamprec, B. Žinić, Synthesis and antitumor activity of 5-bromo-1-mesylyracil, *Nucleos. Nucleot. Nucl.* **2005**, *24*, 557–569.
- [7] F. Supek, M. Kralj, M. Marjanović, L. Šuman, T. Šmuc, I. Krizmanić, B. Žinić, Atypical cytostatic mechanism of *N*-1-sulfonylcytosine derivatives determined by *in vitro* screening and computational analysis, *Invest. New Drugs* **2008**, *26*, 97–110.
- [8] Lj. Glavaš-Obrovac, I. Karner, M. Štefanić, J. Kašnar-Šamprec, B. Žinić, Metabolic effects of novel *N*-1-sulfonylpyrimidine derivatives on human colon carcinoma cells, *Il Farmaco* **2005**, *60*, 479–483.
- [9] J. Kašnar-Šamprec, Lj. Glavaš-Obrovac, M. Pavlak, N. Štambuk, P. Konjevoda, B. Žinić, Spectroscopic characterization and biological activity of *N*-1-sulfonylcytosine derivatives, *Croat. Chem. Acta*, **2005**, *78*, 261–267.
- [10] M. Pavlak, R. Stojković, M. Radačić-Aumiler, J. Kašnar-Šamprec, J. Jerčić, K. Vlahović, B. Žinić, M. Radačić, Antitumor activity of novel *N*-sulfonylpyrimidine derivatives on the growth of anaplastic mammary carcinoma *in vivo*, *J. Cancer Res. Clin. Oncol.* **2005**, *131*, 829–836.
- [11] J. Kašnar-Šamprec, I. Ratkaj, K. Mišković, M. Pavlak, M. Baus-Lončar, S. Kraljević Pavelić, Lj. Glavaš-Obrovac, B. Žinić, *In vivo* toxicity study of *N*-1-sulfonylcytosine derivatives and their mechanisms of action in cervical carcinoma cell line, *Invest. New Drugs* **2012**, *30*, 981–990.
- [12] H.L. Singh, J. Singh, A. Mukherjee, Synthesis, spectral, and *in vitro* antibacterial studies of organosilicon(IV) complexes with schiff bases derived from amino acids, *Bioinorg. Chem. Appl.* **2013**, 2013.
- [13] N. Gokhale, S. Padhye, D Rathbone, D. Billington, P. Lowe, C. Schwalbe, C. Newton The crystal structure of first copper(II) complex of a pyridine-2-carboxamidrazone - a potential antitumor agent. *Inorg. Chem. Commun.* **2001**, *4*, 26–29.
- [14] Lj. Glavaš-Obrovac, M. Jukić, K. Mišković, I. Marković, D. Saftić, Ž. Ban, J. Matić, B. Žinić, Antiproliferative and proapoptotic activity of molecular copper(II) complex of *N*-1-tosylcytosine, *J. Trace Elem. Med. Biol.* In press, doi: 10.1016/j.jtemb.2017.10.009
- [15] A. Višnjevac, M. Luić, R. Kobetić, D. Gembarovski, B. Žinić, Stabilization of the *N*-1-substituted cytosinate iminooxo form in dinuclear palladium complexes. *Polyhedron*, **2009**, *28*, 1057–1064.
- [16] R. Kobetić, D. Gembarovski, A. Višnjevac, B. Žinić, V. Gabelica-Marković, ESI MS Studies of Palladium (II) Complexes with 1-(*p*-Toulenesulfonyl)cytosine/cytosinato Ligands. *J. Mass.Spectrom.*, **2010**, *45*, 51–64.
- [17] A. Višnjevac, N. Biliškov, B. Žinić, Transition metal complexes of *N*-1-tosylcytosine and *N*-1-mesylycytosine. *Polyhedron*, **2009**, *28*, 3101–3109.
- [18] V. Ključarić, R. Kobetić, J. Rinkovec, S. Kazazić, D. Gembarovski, D. Saftić, J. Matić, Ž. Ban, B. Žinić, ESI-MS studies of the non-covalent interactions between the biologically important metal ions and *N*-sulfonylcytosine derivatives, *J. Mass Spectrom.*, **2016**, *51*, 998–1005.
- [19] L. O. Gerlach, J. S. Jakobsen, K. P. Jensen, M. R. Rosenkilde, R. T. Skerlj, U. Ryde, G. J. Bridger, T. W. Schwartz, Metal Ion Enhanced Binding of AMD3100 to Asp²⁶² in the CXCR4 Receptor, *Biochem.*, **2003**, *42*, 710.

- [20] X. Liang, P. J. Sadler, Cyclam complexes and their applications in medicine, *Chem. Soc. Rev.*, **2004**, *33*, 246.
- [21] L. O. Gerlach, J. S. Jakobsen, K. P. Jensen, M. R. Rosenkilde, R. T. Skerlj, U. Ryde, G. J. Bridger, T. W. Schwartz, Metal Ion Enhanced Binding of AMD3100 to Asp²⁶² in the CXCR4 Receptor, *Biochem.*, **2003**, *42*, 710.
- [22] X. Liang and P. J. Sadler, Cyclam complexes and their applications in medicine, *Chem. Soc. Rev.*, **2004**, *33*, 246.
- [23] M. Yu, G. Nagalingam, S. Ellis, E. Martinez, V. Sintchenko, Nontoxic Metal–Cyclam Complexes, a New Class of Compounds with Potency against Drug-Resistant Mycobacterium tuberculosis; *J. Med. Chem.* **2016**, *59*, 5917–5921.
- [24] V. Félix, T.M. Santos, J. Madureira, F. Mirante, S. Quintal, B.J. Goodfellow, M.G. Santana-Marques, J. Pedrosa de Jesus, M.G.B. Drew, M.J. Calhorda, Structural characterization and DFT studies of [Cr(cyclam)(O-dmsO)Cl]₂C: a new precursor complex towards potential DNA intercalators. *Inorg. Chim. Acta* **2003**, *356*, 335; P.V. Bernhardt, E.J. Hayes. Crown ether appended cyclam receptors for cationic guests. *Inorg. Chem.* **2002**, *41*, 2892; H.A.A. Omar, P. Moore, N.W. Alcock. Preparation and characterisation of Organocobalt(III) complexes of tetraaza macrocyclic ligands. Crystal structures of ethyl- and propyl-cobalt(III) complexes of 3,7,11,17-tetraazabicyclo[11.3.1]heptadeca-1(17),13,15- triene. *J. Chem. Soc., Dalton Transactions* **1994**, *18*, 2631; E. Simon, P. L'Haridon, M. L'Her Electrochemical, spectrochemical characterization and crystal structure of (1,4,8,11- tetrazacyclotetradecane)(acetylacetonate) cobalt(III) complexes. *Inorg. Chim. Acta* **1998**, *282*, 173; D. Parker, P.S. Roy. Solution behaviour of a monooxorhenium(V) complex of 1,4,8,11-tetraazacyclo-tetradecane. *Inorg. Chim. Acta* **1988**, *148*, 251.
- [25] R. Colton, S. Mitchell, J.C. Traeger. Interactions of some crown ethers, cyclam and its tetrathia analogue with alkali, alkali earth and other metal ions: an electrospray mass spectrometric study. *Inorg. Chim. Acta* **1995**, *231*, 87.
- [26] I. Alfonso, C. Astorga, V. Gotor Electrospray ionization mass spectrometry (ESI-MS) as a useful tool for fast evaluation of anion and cation complexation abilities of a cyclam derivative. *Journal of Inclusion Phenomena and Macrocyclic Chemistry* **2005**, *53*, 131.
- [27] E.S. Baker, J.E. Bushnell, S.R. Weckler, M.D. Lim, M.J. Manard, N.F. Dupuis, P.C. Ford, Bowers MT. Probing shapes of bichromophoric metal-organic complexes using ion mobility mass spectrometry *J. Am. Chem. Soc.* **2005**; *127*, 18222.
- [28] T. Felder, A. Röhrich, H. Stephan, C. A. Schalley, Fragmentation reactions of singly and doubly protonated thiourea- and sugar-substituted cyclams and their transition-metal complexes, *J. Mass Spectrom.* **2008**, *43*, 651–663.
- [29] D. Prukala, New compounds via Mannich reaction of cytosine, paraformaldehyde and cyclic secondary amines *Tetrahedron Lett.* **2006**, *47*, 9045–9047.
- [30] J. Matic, I. Nekola, A. Višnjevac, R. Kobetic, I. Martin-Kleiner, M. Kralj, B. Žinić, C5-Morpholinomethylation of N1-sulfonylcytosines by a one-pot microwave assisted Mannich reaction, *Org. Biomol. Chem.* **2018**, DOI: 10.1039/c8ob00253c.
- [31] W. Yang, C. M. Giandomenico, M. Sartori, D. A. Moore, Facile N-1 protection of cyclam, cyclen and 1,4,7-triazacyclononan, *Tetrahedron Lett.* **2003**, *44*, 2481.
- [32] K. B. Sloan and K. G. Silver, The aminomethylation of adenine, cytosine and guanine, *Tetrahedron* **1984**, *40*, 3997.
- [33] Zinc ⁶⁴Zn: 63.93; Copper ⁶³Cu: 62.93; Sodium ²³Na.
- [34] M. Liu, Tingting Li, F. S. Amegayibor, D. S. Cardoso, Y. Fu, J.n K. Lee, Gas-Phase Thermochemical Properties of Pyrimidine Nucleobases, *J. Org. Chem.* **2008**, *73*, 9283–9291; Y. Huang, L. Liu, S. Liu, Toward extension of the gas-phase basicity scale by novel pyridine containing guanidines, *Chemical Physics Letters*, **2012**, *527*, 73-78; G. N. Merrill, G. D. Fletcher, The prediction of gas-phase and aqueous basicities for alkyl amines, *Journal of Molecular Structure: THEOCHEM*, **2008**, *849*, 84-97; S. A. McLuckey, R. G. Cooks, J. E. Fulford, Gas-phase thermochemical information from triple quadrupole mass spectrometers: Relative proton affinities of amines, *International Journal of Mass Spectrometry and Ion Physics*, **1983**, (2–3) *52*, 165-174.

[35] D. P. Demarque, A. E. M. Crotti, R. Vessecchi, J. L. C. Lopesa, N. P. Lopes, Fragmentation reactions using electrospray ionization mass spectrometry: an important tool for the structural elucidation and characterization of synthetic and natural products, *Nat. Prod. Rep.*, **2016**, *33*, 432-455.

Accepted Article

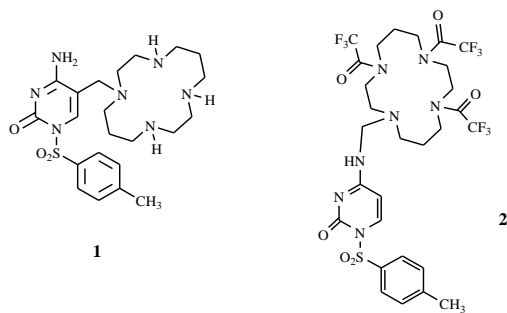


Figure 1. Structures of conjugates **1** and **2**.

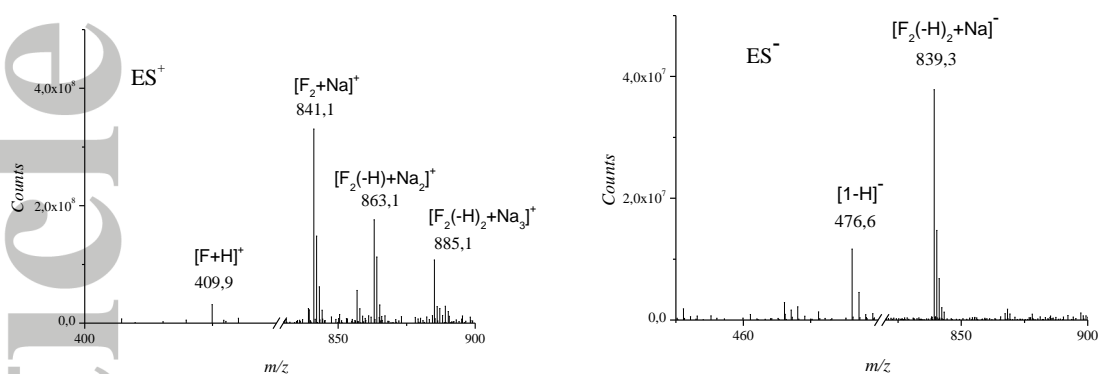


Figure 2. The full scan ESI-MS spectra of a 0.05 mg/mL methanol solution of **1** in both (ES⁺ and ES⁻) modes divided to two m/z regions for clarity. Signals corresponding to fragment **F** and its adducts are the major species observed in ES⁺ mode while the signal of the molecular ion was detected in ES⁻ together with the sodium dimer adduct at m/z 839.3.

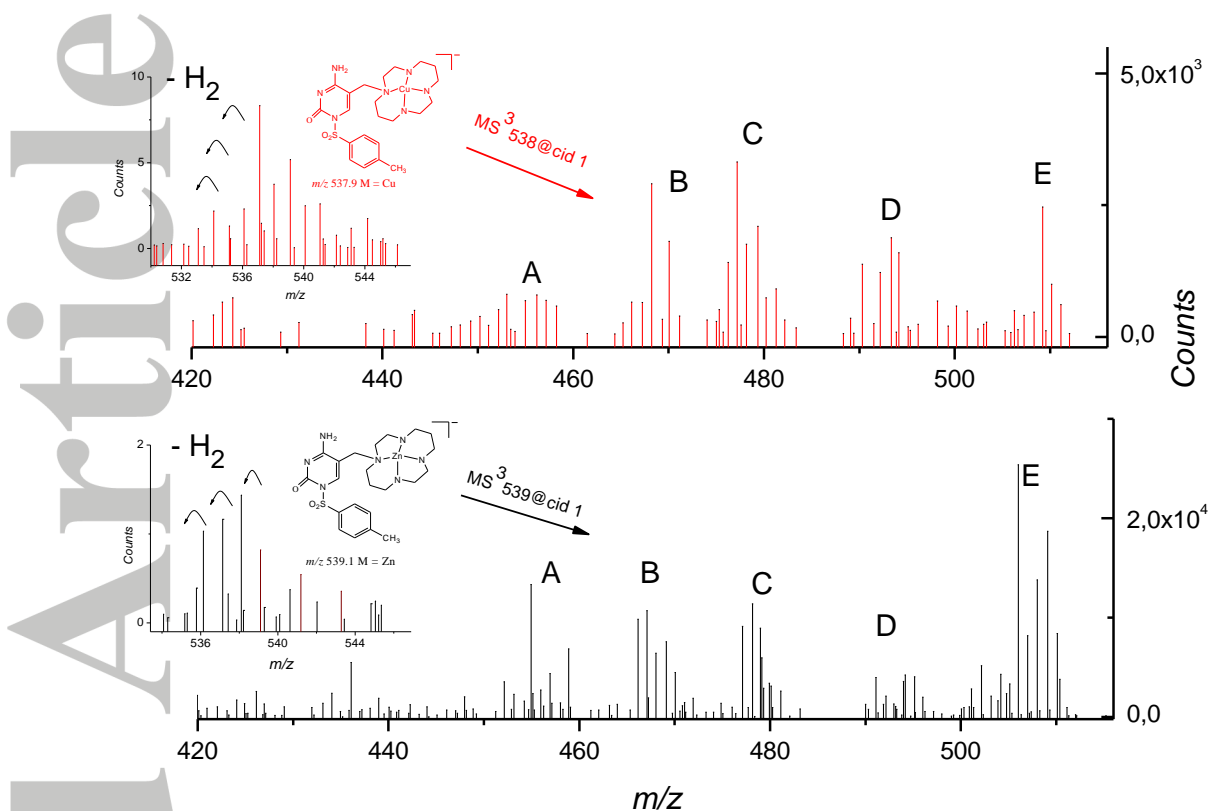


Figure 3. Fragmentation obtained from ESI MS³ studies for the dissociation of the Cu²⁺ complex ion (MS³538 @cid 1) and Zn²⁺ complex ion (MS³539 @cid 1) by selecting a parent ion window of typically 2 amu (i.e. parent mass \pm 1 amu). Selected precursor ions were isolated upon MS² experiment: m/z 537.9 obtained from molecular ion m/z 573 for Cu²⁺ complex ion and m/z 539.1 obtained from molecular ion m/z 1033 for Zn²⁺ complex ion. It could be seen that the collision induced dissociation caused sequential H₂ loses for both kind of complex ions at same applied experimental conditions during the MSⁿ experiments.

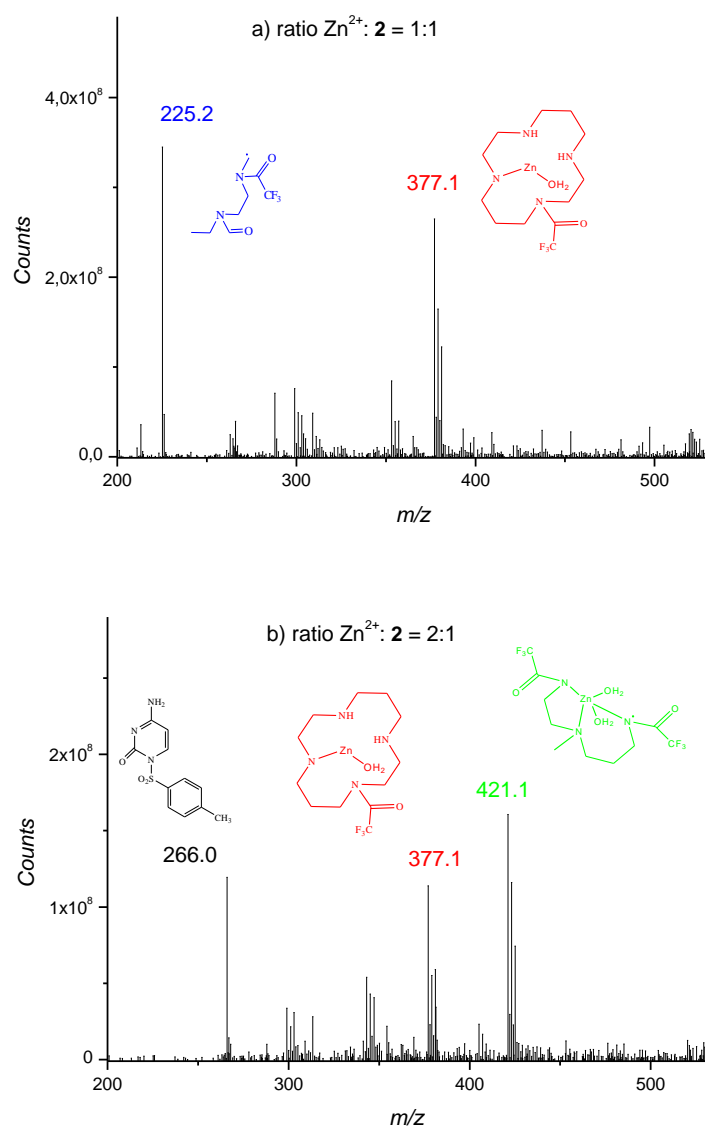


Figure 4. Full scan ES⁺ spectrum for Zn²⁺ complex of compound **2** dissolved in methanol at about 10⁻⁵ M. Major fragments and single-charged Zn²⁺ complex ions observed due to the charge-separating side-chains departures: a) ratio Zn²⁺: **2** = 1:1; b) ratio Zn²⁺: **2** = 2:1.

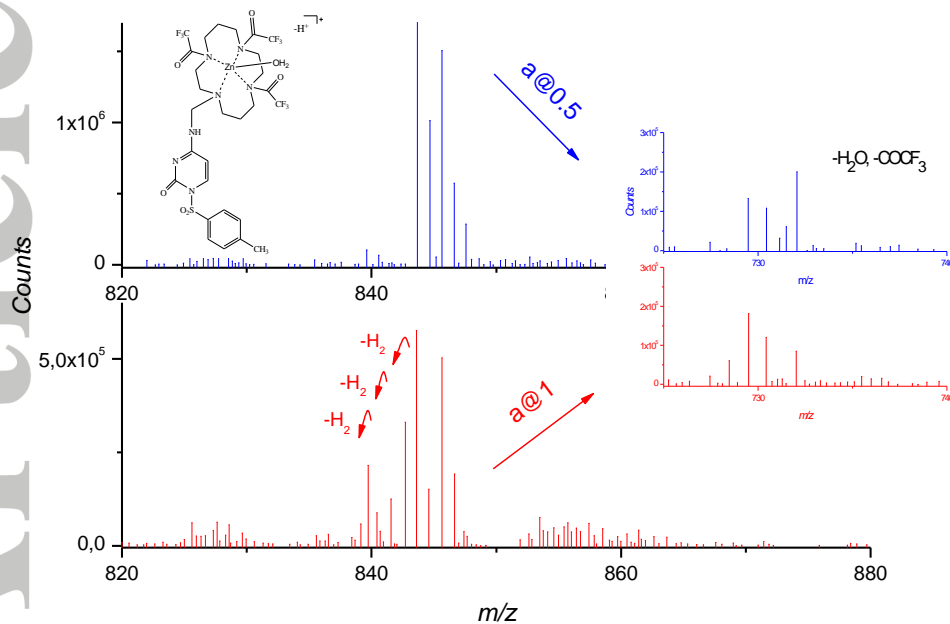
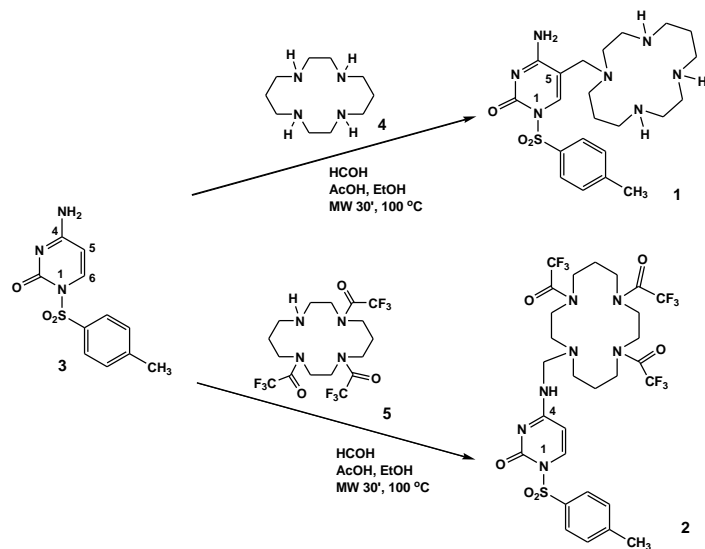
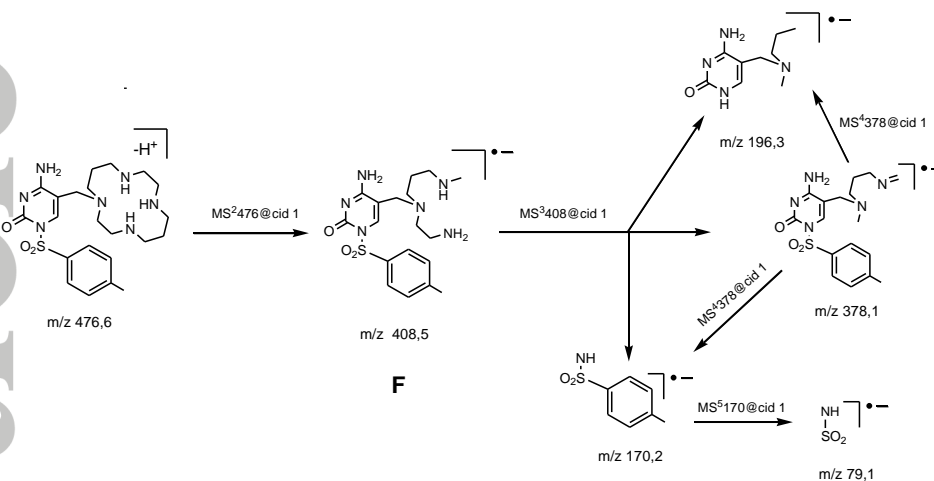


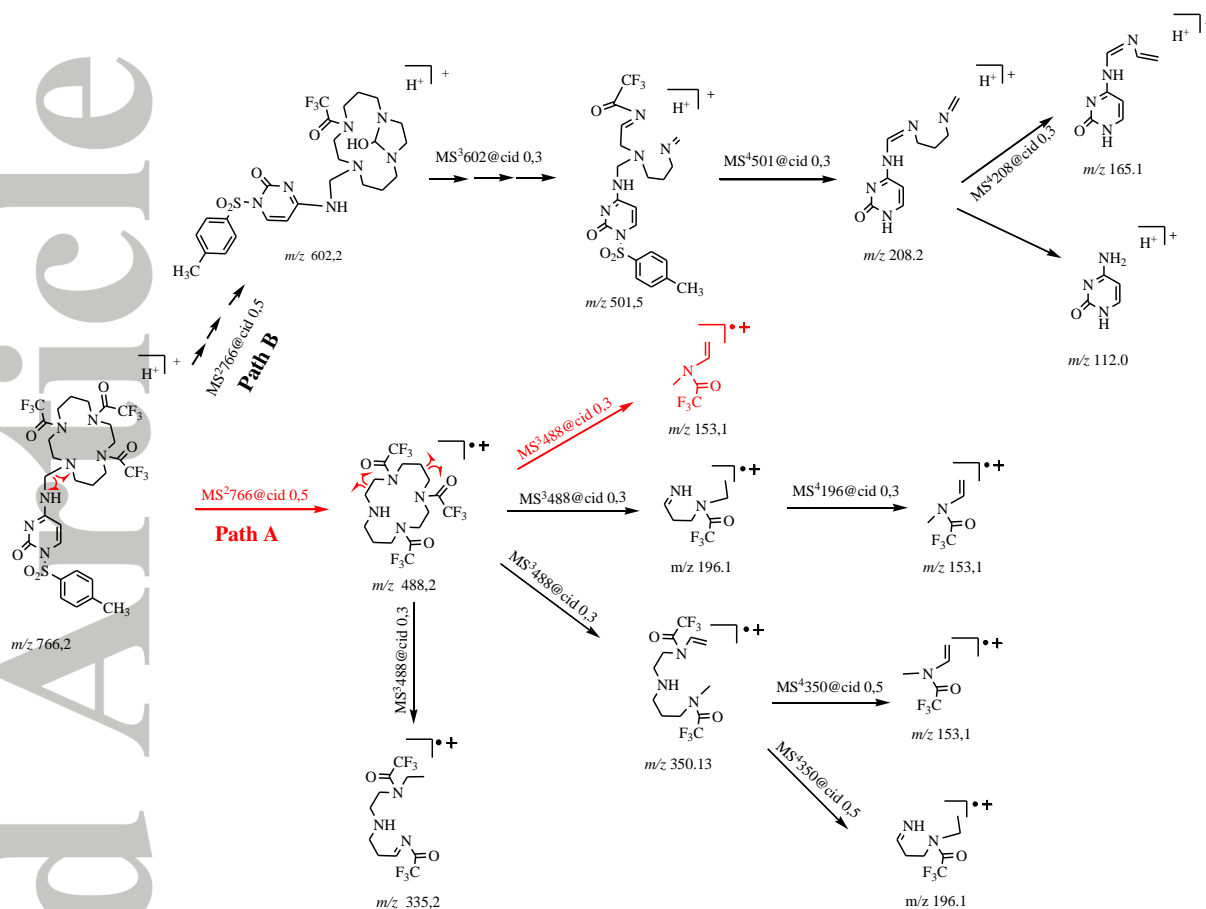
Figure 5. Fraction of the CID mass spectra of mass-selected monoisotopic $[2+Zn^{2+}-H^+]^+$ cation, signal m/z 847 at two different values of CE. Collision induced dissociation caused sequential H_2 loses detected from the single-charged complex ions observed for the isolated ion and for the newly formed species (e.g. inserted signals for the species formed upon elimination of H_2O and $-COCF_3$ group).



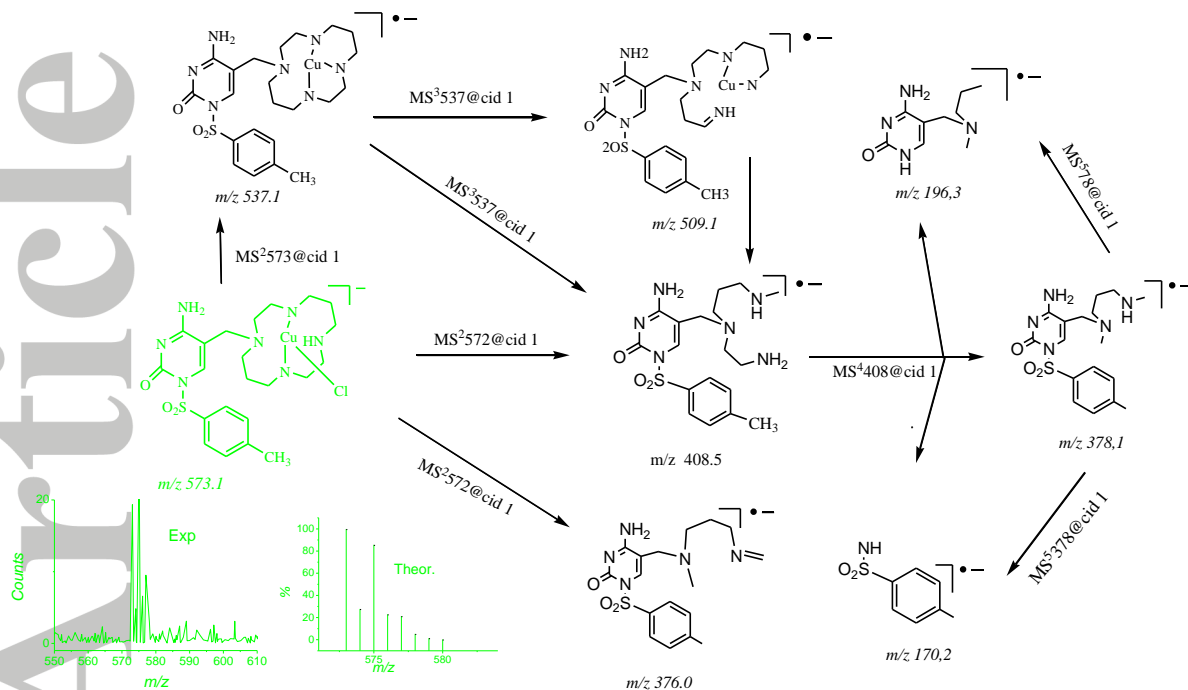
Scheme 1. Synthesis of C- and N-aminomethylated derivatives **1** and **2**.



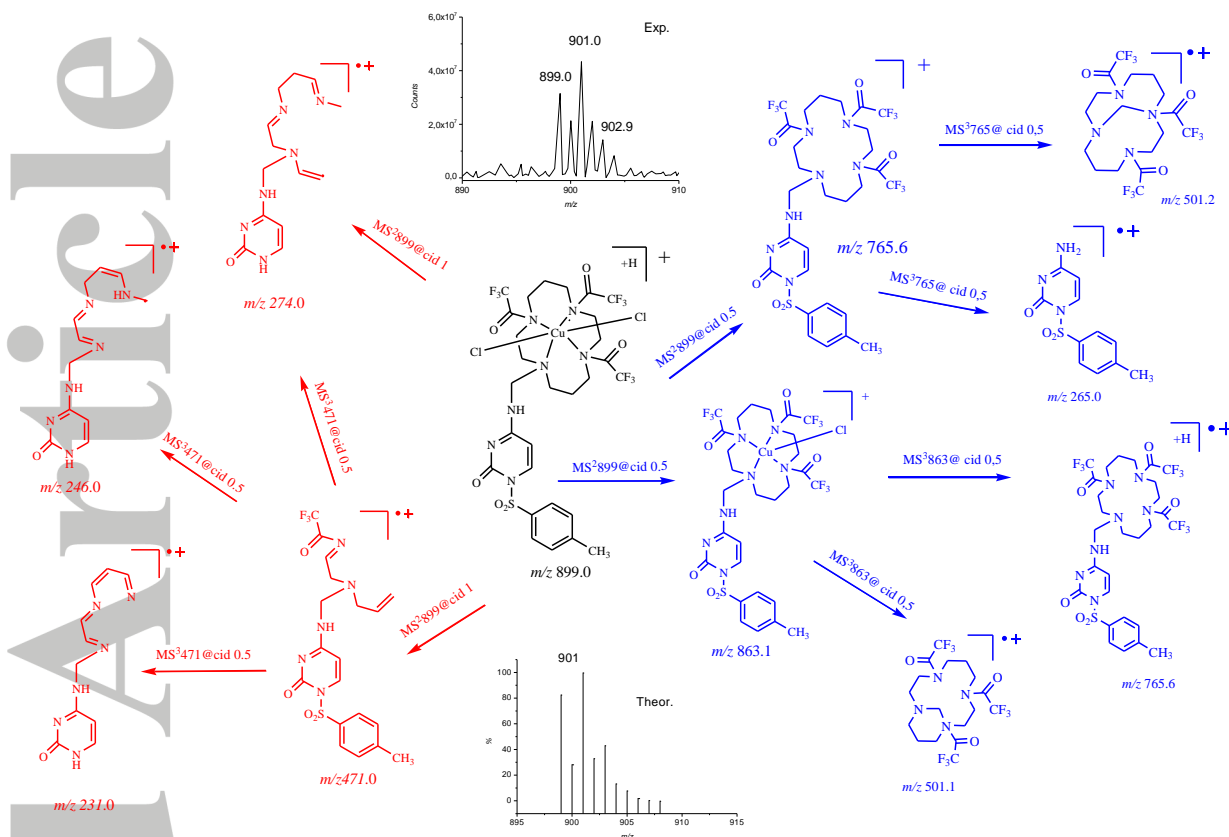
Scheme 2. The fragmentation pathways obtained from ESI MSⁿ studies for the dissociation of the deprotonated molecule **1** observed at *m/z* 476 in ES⁻ mode. The multiple-stage (MSⁿ) CID schemes are based on the CID of the *m/z* 476 peak by selecting a parent ion window of typically 2 amu (i.e., parent mass ±1 amu).



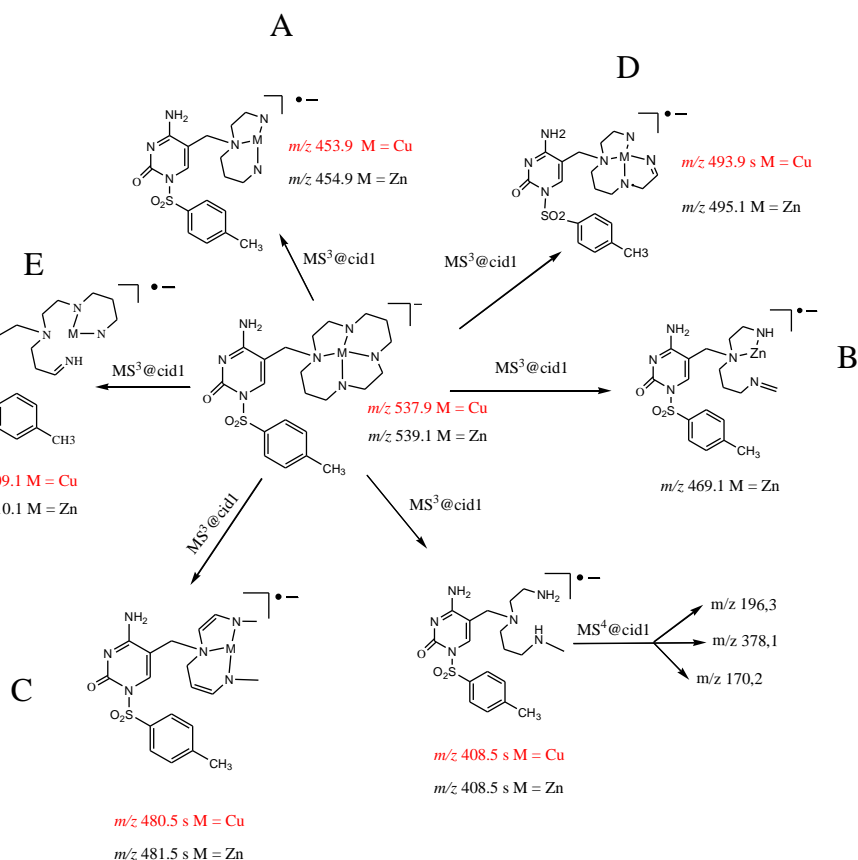
Scheme 3. The fragmentation pathways obtained from ESI MSⁿ studies for the dissociation of the protonated molecule **2** observed at m/z 766 in ES⁺ mode. The multiple-stage (MSⁿ) CID schemes are based on the CID of the m/z 766 peak by selecting a parent ion window of typically 2 amu (i.e., parent mass \pm 1 amu). Path A proceeded through radical fragmentation reactions (one example is red colored), while path B proceeded through several charge-migration fragmentation reactions (initiated by protonation on the carbonyl oxygen). The structures observed as signals with low abundance are omitted in the scheme.



Scheme 4. The fragmentation pathways obtained from ESI MSⁿ studies for the dissociation of the single-charged molecular complex Cu(II) ion of **1** observed at m/z 573 in ES⁻ mode. The multiple-stage (MSⁿ) CID schemes are based on the CID of the m/z 573 peak by selecting a precursor ion window of typically 2 amu (i.e., parent mass \pm 1 amu).



Scheme 5. The fragmentation pathways (at higher CE red, at lower CE blue) obtained from ESI MSⁿ studies for the dissociation of the protonated Cu (II) complex of **2** observed at *m/z* 899 in ES⁺ mode. The multiple-stage (MSⁿ) CID schemes are based on the CID of the *m/z* 899 peak by selecting a precursor ion window of typically 2 amu (i.e., parent mass ±1 amu).



Scheme 6. An example of the fragmentation pathways obtained from ESI MSⁿ studies for the dissociation of the complex ions observed at m/z 537.9 for Cu²⁺ complex ion (MS³538 @cid 1) and at m/z 539.1 for Zn²⁺ complex ion (MS³539 @cid 1). The multiple-stage (MSⁿ) CID schemes are based on the CID of the ⁶³Cu and ⁶⁴Zn isotopic peaks by selecting a precursor ion window of typically 2 amu (i.e., parent mass ±1 amu).